Ruhou Gao
Gas Turbine Laboratory,
Massachusetts Institute of Technology,
Cambridge, MA 02139
e-mail: ruhou@mit.edu

Zoltán Spakovszky[1]
Fellow ASME
Gas Turbine Laboratory,
Massachusetts Institute of Technology,
Cambridge, MA 02139
e-mail: zolti@mit.edu

Daniel Rusch
Compressor Development,
ABB Turbo Systems, Ltd.,
Baden 5400, Switzerland
e-mail: daniel.rusch@ch.abb.com

René Hunziker
Compressor Development,
ABB Turbo Systems, Ltd.,
Baden 5400, Switzerland
e-mail: rene.hunziker@ch.abb.com

Area Schedule Based Design of High-Pressure Recovery Radial Diffusion Systems

High-pressure ratio centrifugal compressors require advanced diffusion systems to achieve enhanced efficiencies set by future turbocharger applications. To address the shortcomings of the commonly used channel diffuser and airfoil cascade design perspectives, a streamtube based area schedule is adopted paying special attention to the diffuser entry region. It is shown that the diffusion in the semivaneless space, controlled chiefly by inlet flow angle and the vane suction side geometry, plays a key role in improving diffuser performance. Removing excess thickness from the suction side eliminates flow overspeed, increases effective diffusion length, and leads to higher pressure recovery at reduced stagnation pressure loss. The pressure side thickness distribution controls the channel area schedule. Thin leading edges (LEs) ensure smooth flow area transition into the channel and reduce the vane upstream influence, mitigating high-cycle fatigue related mechanical issues. [DOI: 10.1115/1.4034488]

Introduction

The complex nature of the impeller outflow presents multiple challenges for the downstream vaned diffuser. More specifically, the impact of flow angle, Mach number, flow nonuniformity, and unsteadiness on diffuser performance was investigated in a companion paper [1]. It was demonstrated through computations and experiment that diffuser performance in terms of effectiveness, which describes the pressure recovery obtained relative to the maximum possible pressure rise, correlates well with the mixed-out averaged impeller outflow angle. It was also shown that, due to strong mixing processes in the diffuser inlet region, effectiveness is largely independent of the time-averaged spanwise and unsteady pitchwise nonuniformity from the impeller. Based on this, careful consideration must be given in the design process to the diffuser inlet region and, from a practical perspective, simplified, isolated diffuser calculations can be adopted given proper definition of the inflow conditions. This is the focus of the present paper.

There are two commonly used design approaches for radial vaned diffusers: the channel diffuser approach and the airfoil (cascade) based approach. Extensive databases in the literature exist for both (see, for example, Refs. [2–5]) and have been used with success. There is, however, a lack of first principles based design guidelines which could possibly break new ground in further advancing diffuser performance. The former approach considers the radial vaned diffuser to be similar to a straight-walled channel diffuser. The best design is achieved where a balance is struck between the length-to-width ratio and the area ratio (AR). The challenge is that the vane inlet and exit metal angles are important in impeller and volute matching but are not accounted for. Also, there is a lack of consistency in the definition of diffuser area ratio which is complicated by the geometry of the semibounded space in the diffuser entry region, commonly denoted as the semivaneless space (SVLS).

An alternative perspective is the airfoil cascade approach which uses a conformal transformation of linear cascade data into the radial plane [6]. While the metal angles are well defined for component matching, estimating stagnation pressure loss becomes a challenging task because the linear cascade data do not account for the increase in area with radius. Put another way, a separation-free linear cascade design might cause severe separation after conformal transformation. To account for this, typically a factor of 7 or 8 in loss coefficient is recommended when estimating stagnation pressure loss using linear cascade data [4]. Finally, both channel diffuser and airfoil cascade design approaches neglect the strong mixing and diffusion in the vaneless and the semivaneless space which, as will be shown, are the key design considerations.

The centrifugal compressor investigated here is a 5.0 pressure ratio, high-speed compressor of advanced design with an impeller blade Mach number of 1.54. As sketched in Fig. 1, the test article consists of an impeller and a vaned diffuser (together called the stage) and a volute. The impeller contains nine main and nine splitter blades with backsweep, and the vaned diffuser consists of 17 aerodynamically profiled vanes. In the blade-to-blade domain, the vaned diffuser can be divided into the following five subcomponents, as shown in Fig. 2: (1) *vaneless space* (VLS): unbounded flow path where diffusion is mainly set by endwall contour (pinch) and impeller exit flow angle, (2) *semivaneless space* (SVLS): semibounded flow path where diffusion is mainly governed by the vane suction side geometry, (3) *channel*: diffusion is mainly set by area ratio and length-to-width ratio, following classical channel diffuser guidelines, (4) *downstream* SVLS: diffusion is mainly set by vane exit angle and vane pressure side, and (5) *downstream* VLS: diffusion is mainly set by swirl angle and radius ratio.

Given the impeller outflow angle, endwall contour, and profiled vane diffuser geometry,[2] the area schedule can be calculated and is shown in Fig. 2 on the bottom. The suction side of the vane near the leading edge, set by the camberline and thickness distribution, decreases the flow area in the SVLS and leads to flow acceleration, reducing diffusion and effective diffuser length and yielding flow separation and reduced pressure recovery.

[1]Corresponding author.

Contributed by the International Gas Turbine Institute (IGTI) of ASME for publication in the JOURNAL OF TURBOMACHINERY. Manuscript received August 1, 2016; final manuscript received August 9, 2016; published online September 27, 2016. Editor: Kenneth Hall.

[2]From here on, this diffuser geometry will be referred to as the baseline diffuser.

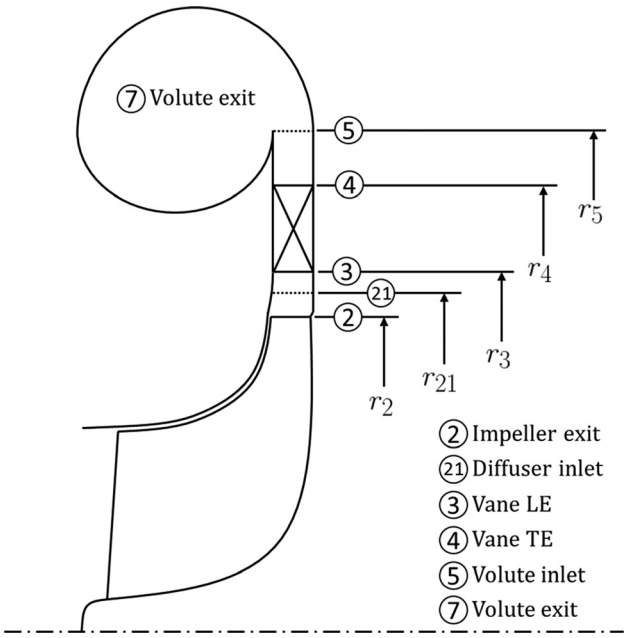

Fig. 1 Meridional view of centrifugal compressor

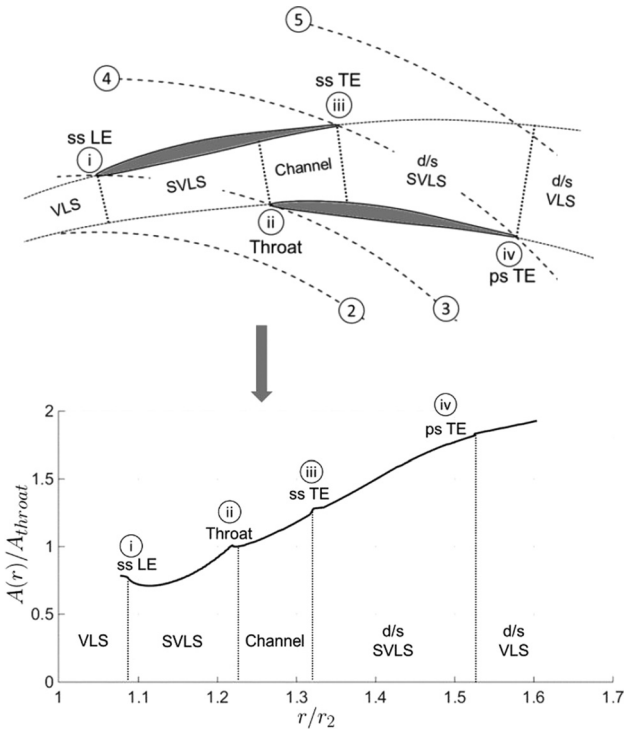

Fig. 2 Illustration of a typical vaned diffuser and its subcomponents (top) and flow area distribution as a function of radius (bottom)—note flow acceleration and therefore reduced diffusion in semivaneless space (SVLS)

Scope of Paper

In the quest of identifying a vane geometry with significantly improved performance, the idea is to adopt a streamtube perspective and to define the vane suction and pressure sides by a carefully scheduled flow area distribution that maximizes diffusion while keeping stagnation pressure loss at a minimum. Special attention is given to the diffuser entry region, with consideration of mixing and high diffusion in the vaneless and semivaneless space. The objective is to determine the best area schedule, and

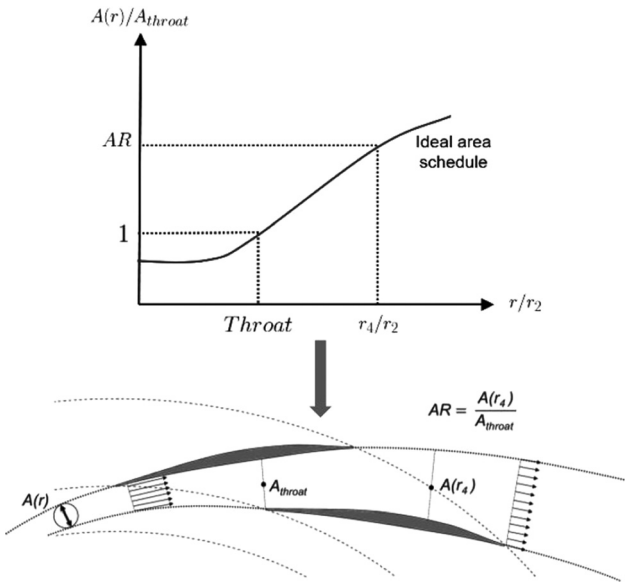

Fig. 3 Aft-thickened vaned diffuser geometry defined by an ideal area schedule and high loading in the semivaneless space

therefore vane geometry, given properly averaged impeller exit conditions. More specifically, this paper addresses the following research questions:

(1) For a given impeller outflow and infinitely thin vanes, what is the ideal diffuser performance and corresponding area schedule?
(2) Given this ideal diffusion path, what thickness distribution yields minimum impact on performance while meeting structural requirements?
(3) What is the impact of such an improved diffuser design on impeller and volute performance?

The investigation begins with the assumption that zero-thickness vanes yield the best performance. This assumption will be verified later. Further, it will be shown in both computations and full-scale compressor experiments that aft-thickened vanes, defined by a smooth and continuous area schedule with high loading in the semivaneless space (see Fig. 3), yield close to a doubling in the ratio of pressure recovery over stagnation pressure loss. A shorter vaneless space, enabled by thin vane leading edges, avoids flow acceleration and improves diffusion in the semivaneless space. The closer-spaced diffuser vanes increase impeller efficiency by 0.8% points while almost halving the upstream influence. The aim of this paper is to lay out step by step the general process and guidelines by which vaned diffuser performance is improved. Implications on the matching of upstream and downstream components, such as the volute, are also discussed.

Technical Approach

The same impeller and diffuser endwall contour, including pinch, were used throughout this study. All the investigations were carried at impeller design speed, and the diffuser throat area was maintained for all the geometries so as to keep the same flow capacity [7]. Furthermore, the diffuser inlet metal angles were matched to the impeller outflow at zero incidence.[3]

First, zero-thickness vaned diffusers, so-called camberline diffusers, were defined and assessed in a parametric study to identify the ideal diffusion path, characterized by diffuser inlet and exit radius ratios and vane turning angle, $\alpha_4 - \alpha_3$. Next, the vane profile thickness distribution and leading edge geometry were

[3]A one-dimensional compressible channel flow model was used in the vaneless space. A detailed description can be found in Ref. [8].

systematically varied to assess their impact on diffuser performance. Finally, the calculations were compared and validated with full-scale compressor experiments.

Three different diffuser designs using the area scheduling approach were assessed in a turbocharger compressor test facility at ABB Turbo Systems, Ltd., Baden, Switzerland. The stage performance was calculated by a proprietary mean-line data reduction scheme. The diffuser subcomponent performance was dissected using an array of pressure taps located on the shroud side endwall.

Steady impeller–diffuser Reynolds-averaged Navier–Stokes (RANS) calculations were performed in NUMECA FINE/Turbo using the same setup as in Ref. [1]. For a single passage calculation, typical node numbers for the impeller and the diffuser meshes were 1.4 and 0.4×10^6, respectively. The Spalart–Allmaras turbulence model was used with y^+ values maintained between 1 and 10. All the calculations were performed at standard day +10 °C conditions. The flow conditions at diffuser inlet, r_{21}, and exit, r_{41}, were extracted at a distance of 7.5% and 52% of impeller exit radius, respectively. Mixed-out averaged flow conditions were used in the assessment and show good agreement with the time and area averaged flow conditions obtained in the experiments.

Compression system performance was assessed via machine isentropic efficiency. To characterize vaned diffuser performance, static pressure recovery and total pressure loss coefficients were defined as

$$C_p = \frac{p_5 - p_2}{p_{t2} - p_2} \tag{1}$$

$$C_{p,t} = \frac{p_{t2} - p_{t5}}{p_{t2} - p_2} \tag{2}$$

Similar to the lift-to-drag ratio, a unified diffuser performance parameter can be defined as

$$\frac{C_p}{C_{p,t}} = \frac{p_5 - p_2}{p_{t2} - p_{t5}} \tag{3}$$

To decouple the impact of diffuser inlet Mach number, it is useful to also define effectiveness, which relates actual diffuser C_p to the isentropic pressure recovery, $C_{p,i}$

$$\varepsilon_D = \frac{C_p}{C_{p,i}} \tag{4}$$

With a little algebra, the unified diffuser performance parameter and effectiveness can be related via the diffuser exit Mach number

$$\varepsilon_D = \left[1 + \frac{C_{p,t}}{C_p}\left(1 + \frac{\gamma - 1}{2} M_5^2\right)^{\frac{-\gamma}{\gamma - 1}}\right]^{-1} \tag{5}$$

Since $M_5 = M_5(M_2, \mathrm{AR})$, effectiveness is appropriate when comparing diffusers with the same area ratio. When area ratio is a design parameter, diffusers optimized based on ε_D will in general yield lower area ratio and higher residual kinetic energy compared to an optimized design based on $C_p/C_{p,t}$ because of the effect of density change through the diffuser at higher Mach number.

On the other hand, when comparing diffusers with different area ratios for a fixed diffuser inlet Mach number, the appropriate diffuser performance parameter is $C_p/C_{p,t}$. Depending on the design context, both performance metrics are used in this work.

Ideal Diffusion Path

A series of candidate zero-thickness diffusers were designed with circular leading and trailing edges (TEs), and a thin[4] and constant thickness distribution with the aim to establish the link between area ratio and nondimensional diffusion length. In the vaned diffuser design context, the area ratio is controlled by the turning angle, which is the difference between inlet and outlet metal angles, $\alpha_4 - \alpha_3$. The diffuser exit radius ratio, r_4/r_2, mainly characterizes the nondimensional diffusion length. The effect of impeller–diffuser spacing on diffuser performance is investigated by varying the diffuser inlet radius ratio, r_3/r_2. The impact of these three design parameters on diffuser area schedule is schematically illustrated in Fig. 4.

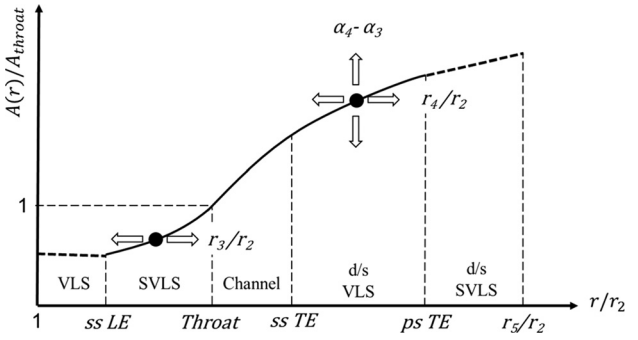

Fig. 4 For a given impeller geometry and fixed throat area, the diffuser area schedule is altered via changes in diffuser inlet and outlet radius ratios and turning

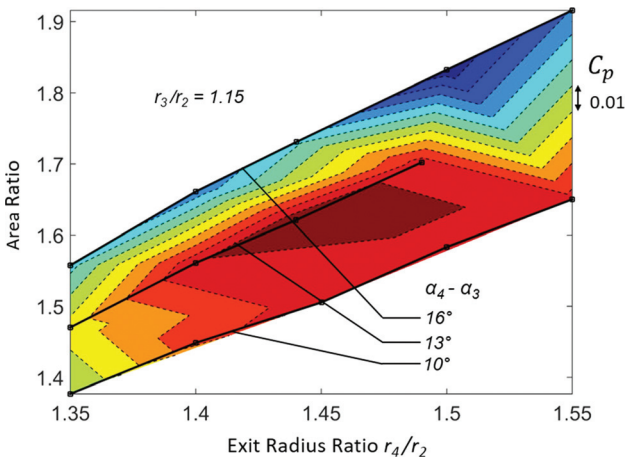

Fig. 5 Static pressure recovery C_p of camberline diffusers with $r_3/r_2 = 1.15$. Highest pressure recovery observed for 13 deg turning.

Based on this, a total of 43 different geometries were assessed using steady-stage calculations. Following the format of a typical Reneau chart, the pressure recovery is assessed as a function of area ratio[5] and nondimensional diffusion length in terms of r_4/r_2 in Fig. 5. The lines of constant turning angles (similar to the divergence angle 2θ in a Reneau chart) are also identified. Maximum C_p is achieved for $1.4 < r_4/r_2 < 1.5$ and AR ≈ 1.6 which is lower than the best AR of 2 and L/W of 8 in a typical Reneau chart. Large increases in flow area and high turning angles at low exit radius ratios can lead to endwall separation reducing the effective flow area and therefore diffusion. In contrast, the stagnation pressure loss coefficient in Fig. 6 increases monotonically with exit radius ratio, as profile loss and the extent of corner separations scale with vane surface area. Without considering the volute, the ideal diffuser area schedule is identified by the ratio of the two parameters, $C_p/C_{p,t}$, in Fig. 7 for $r_4/r_2 \approx 1.4$ and AR ≈ 1.45.

[4]In the calculations, the thickness-to-chord ratio was 1×10^{-6}, effectively removing the effect of thickness distribution on flow area.

[5]In the following figures 5–9, area ratio is defined as $A(r_4)/A_{\mathrm{throat}}$ per Fig. 3.

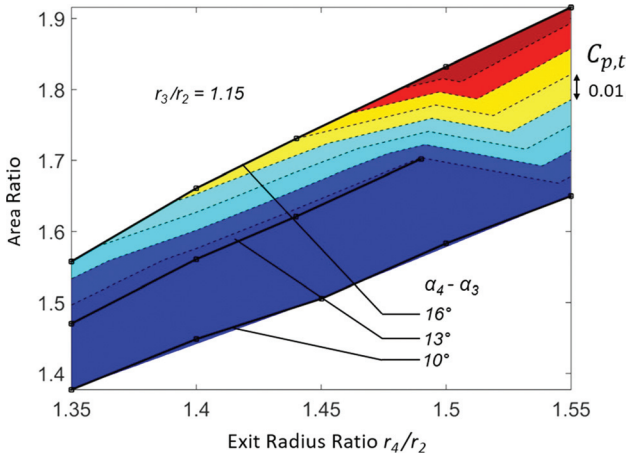

Fig. 6 Stagnation pressure loss $C_{p,t}$ of camberline diffusers with $r_3/r_2 = 1.15$. Diffusers with short diffusion path and moderate area ratio yield lowest loss.

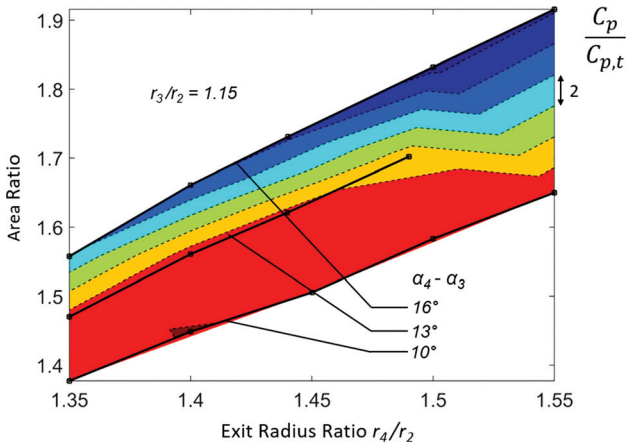

Fig. 7 Performance parameter $C_p/C_{p,t}$ of camberline diffusers with $r_3/r_2 = 1.15$

To characterize the effect of inlet radius ratio on diffuser performance, four different diffuser designs with the same optimum turning angle, area ratio, and chord length were assessed. The comparison in Fig. 8 indicates that closer-spaced diffusers improve diffuser performance. For typical transonic and high swirl impeller exit conditions, the one-dimensional compressible

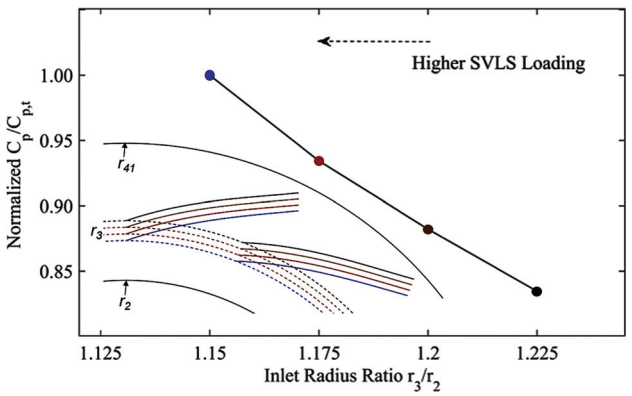

Fig. 8 Strong dependence of diffuser performance parameter $C_p/C_{p,t}$ on diffuser inlet radius ratio governed by diffusion in SVLS

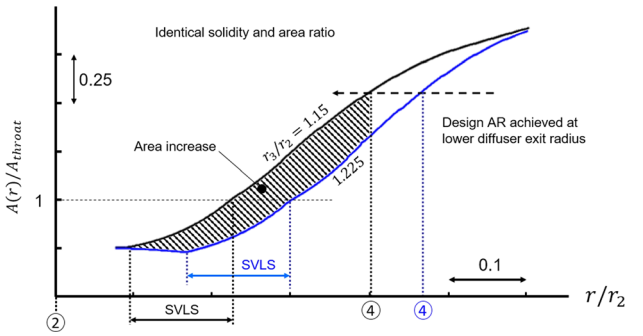

Fig. 9 A closer-spaced semivaneless space improves diffusion and achieves the desired area ratio at lower exit radius ratio

vaneless space flow model [8] suggests a drop in pressure rise upstream of the semivaneless space. In agreement with Ref. [1], a closer-spaced semivaneless space increases the diffuser inlet Mach number and therefore improves diffuser pressure recovery. This also enables a more compact stage design where the desired area ratio can be achieved at a lower exit radius ratio and with a smoother area schedule as shown in Fig. 9. The minimum impeller–diffuser spacing is constrained by mechanical considerations, such as impeller high-cycle fatigue (HCF). To facilitate closer spacing of nonzero thickness vanes, the vane upstream influence must be reduced which will be discussed in detail later.

Volute Matching

Before considering the effects of vane thickness, it is important to characterize the impact of the diffuser exit conditions on volute performance. To achieve a performance improvement on the overall diffusion system level, the diffuser performance charts must be matched to the volute characteristics. Assuming the downstream vaneless space is long enough such that volute is aerodynamically decoupled, a one-dimensional volute model based on diffuser exit conditions can be used to estimate the system level performance. The volute inlet swirl parameter, $\lambda = v_\theta/v_r$, and the volute inlet Mach number have the strongest influence on volute performance. The impact of diffuser geometry on these two parameters is depicted in Figs. 10 and 11. The region of minimum Mach number overlaps with the region of maximum C_p in Fig. 5, and the lowest volute inlet swirl parameter is observed in the same region, causing a more radial flow into the volute. As suggested by typical one-dimensional volute loss models [4], a lower volute inlet swirl

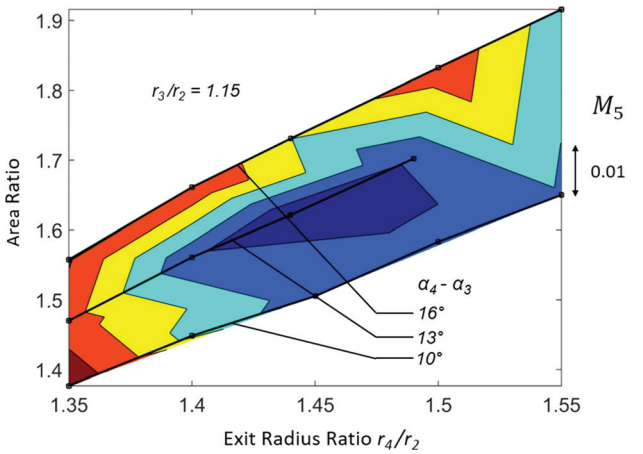

Fig. 10 Exit Mach number of camberline diffusers with $r_3/r_2 = 1.15$. Minimum exit Mach number coincides with maximum C_p in Fig. 5.

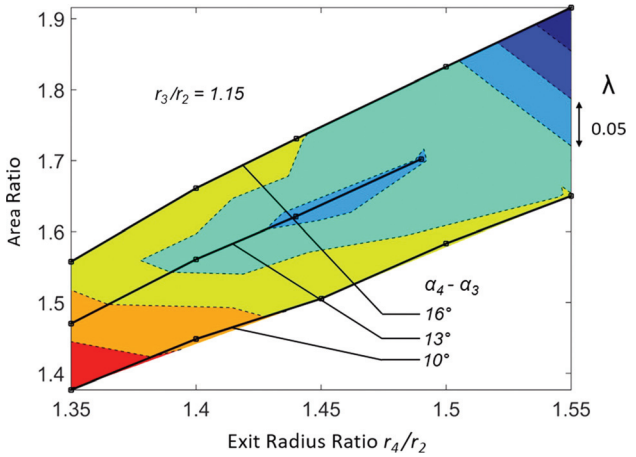

Fig. 11 Mixed-out volute inlet swirl parameter λ of camberline diffusers with $r_3/r_2 = 1.15$. Lowest exit swirl parameter coincides with highest C_p in Fig. 5.

parameter yields higher radial kinetic energy loss in the volute, decreasing volute performance. For a fixed endwall contour, the impact of volute inlet Mach number must therefore be carefully balanced by that of the inlet swirl parameter. While the minimum diffuser exit Mach number is set by diffuser pressure recovery, the system performance can be further improved by profiling the diffuser exit endwall to facilitate a near optimum volute inlet swirl parameter.

Effect of Vane Thickness Distribution

Diffuser performance is sensitive to the suction side geometry because of its strong impact on the area schedule in the semivaneless space. The pressure side, on the other hand, has no impact on flow area up until the diffuser channel. By adopting the ideal camberline as the suction side of the profiled diffuser with nonzero thickness, the SVLS area schedule can be matched to that of the ideal camberline diffuser. To investigate the effect of the channel area schedule on diffuser performance, two different diffuser geometries were assessed using steady RANS calculations. The so-called front-thickened diffuser is a profiled diffuser with the suction side adopted from the ideal camberline diffuser and the pressure side formed by adding the thickness distribution of a controlled diffusion airfoil. The thickness distribution of a NACA SC(2)-1006 supercritical airfoil was chosen for this study. In contrast, the aft-thickened diffuser has the same suction side, but the majority of the vane thickness is introduced at higher radii. The thickness distribution of the aft-thickened diffuser was prescribed by a Gaussian distribution

$$G(x) = e^{-\frac{1}{2}\left(\frac{x-m}{\sigma}\right)^2} \tag{6}$$

where m is the location of maximum thickness, and σ depends on the leading edge thickness. Profiled diffusers with Gaussian thickness distributions will be referred to as G-series diffusers. Figure 12 compares the thickness distributions and the vane geometries of the front and aft-thickened diffusers.

The area schedule of the front and aft-thickened diffusers are compared to the ideal camberline diffuser in Fig. 13. The area schedules in the semivaneless space are nearly identical to that of the ideal camberline diffuser but at diffuser channel inlet, the front-thickened vane experiences a sudden area reduction due to the thick leading edge. In contrast, the aft-thickened vane yields a smoother area transition.

The performance parameter $C_p/C_{p,t}$ of both diffusers and that of the baseline and the ideal camberline diffusers is computed in Fig. 14. In the case of the front-thickened diffuser, peak

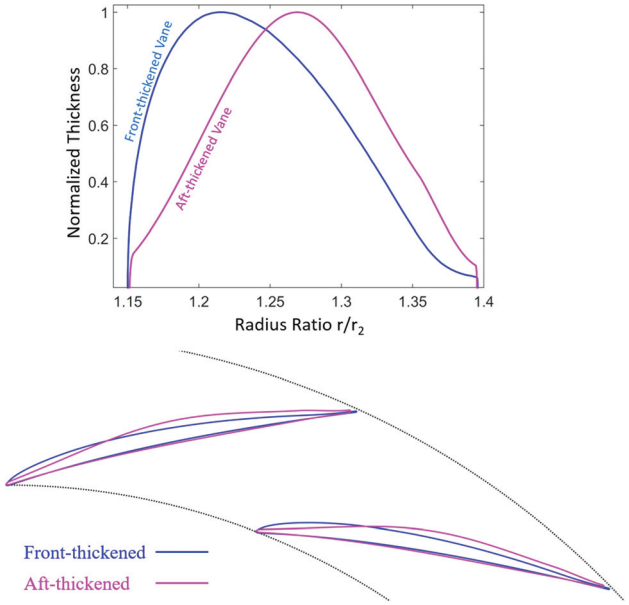

Fig. 12 Top: normalized profile thickness distribution, front versus aft-thickened vanes—the aft-thickened profile distribution removes thickness in the semivaneless space and instead of a thick leading edge thin, elliptical leading edges are used (not shown here). Bottom: front versus aft-thickened vane geometries—controlled diffusion versus Gaussian diffusion (G-series).

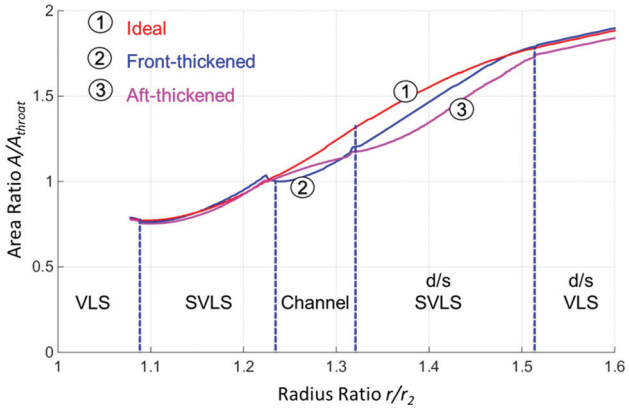

Fig. 13 Comparison of area schedule of the front versus aft-thickened vanes

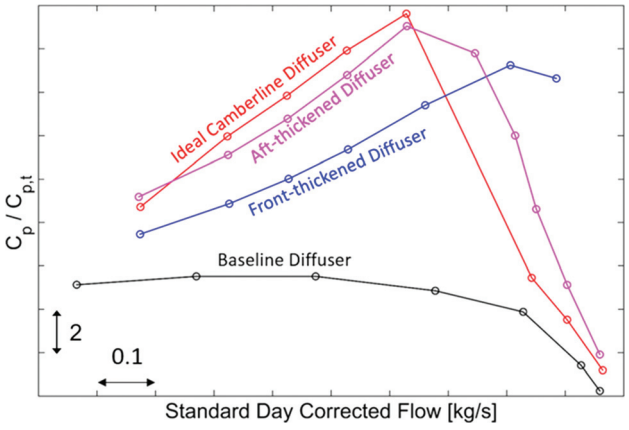

Fig. 14 Performance parameter $C_p/C_{p,t}$ of front and aft-thickened diffuser compared to the baseline and the ideal camberline diffusers

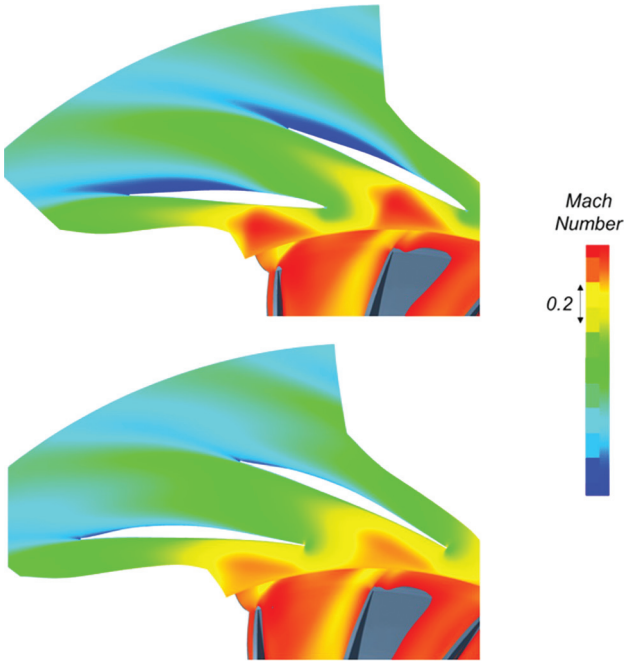

Fig. 15 Mach number contours at midspan at design mass flow: baseline (top) versus aft-thickened G-series diffuser (bottom)

performance is noticeably shifted toward the choke side because for a constant throat area, thickness near the leading edge effectively increases the inlet metal angle toward the radial direction (and thus the flow angle at minimum stagnation pressure loss). This effect is reduced for the aft-thickened diffuser and compared to the baseline diffuser and the front-thickened diffusers with thick leading edges, the aft-thickened diffuser yields characteristics with a distinguished peak. Albeit the undesirable mismatch, there is a marked improvement in performance associated with area scheduling. Eliminating the area reduction in the semivaneless space leads to significant performance improvements in both front and aft-thickened diffusers. Furthermore, by smoothly scheduling the flow area into the diffuser channel, the aft-thickened diffuser performance approaches that of the ideal camberline diffuser.

Returning to the ideal diffuser charts, the elimination of the area reduction in the semivaneless space in the G-series diffusers yields increased effective diffusion length at a given area ratio. This reduces the corner separation as observed in Fig. 15.

Effect of Vane Leading Edge Shape

To assess the impact of vane leading edge thickness on diffuser performance, three diffusers with comparable overall design parameters (r_3/r_2, r_4/r_2, and AR) but different leading edge thicknesses were assessed. The same elliptical leading edge shape, with an eccentricity[6] of 0.95, was used in all the cases. The leading edges were blended into the main vane section ensuring a continuous first derivative of the metal angle at the blending point. The three leading edge geometries are depicted in Fig. 16.

Since the three diffuser geometries have comparable area ratios, effectiveness is the more appropriate metric for performance comparison as it captures the changes in diffuser inlet Mach number. As shown in Fig. 17, increased leading edge thickness markedly reduces diffuser effectiveness. From an area schedule perspective, the leading edge thickness is directly linked to the diffuser

[6]Eccentricity is defined as $\varepsilon = \sqrt{1-(b/a)^2}$, where a and b are the semimajor and semiminor axes of the ellipse.

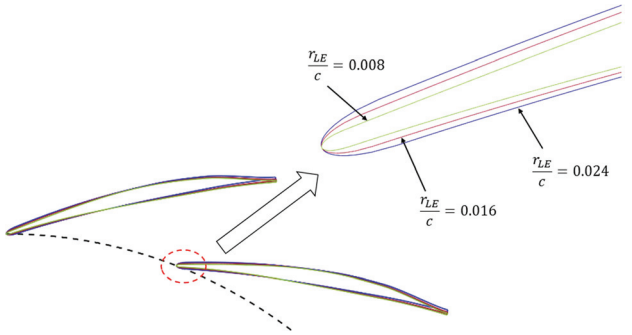

Fig. 16 Comparison of diffuser geometries with different leading edge thicknesses

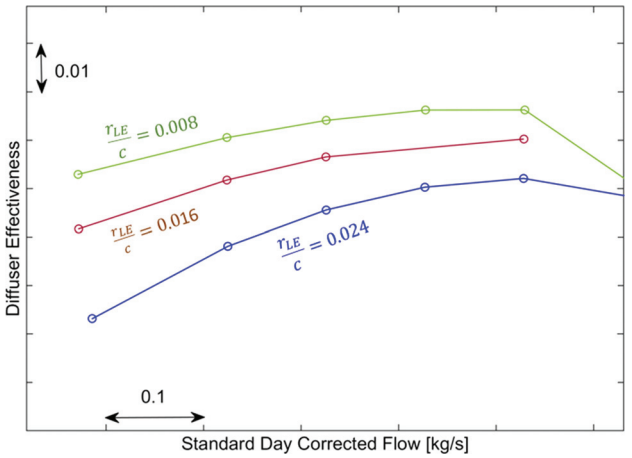

Fig. 17 Impact of diffuser leading edge thickness on diffuser effectiveness. Thicker leading edges lead to more pronounced area reduction at diffuser channel inlet, reducing diffuser effectiveness.

channel flow area schedule. A thicker leading edge leads to a larger flow area reduction at the channel inlet, which causes flow acceleration and decreased pressure recovery.

Vanes with thinner forward portions might be prone to blade wake-induced vibrations. However, the diffuser vanes considered here are clamped between the two diffuser endwall plates so that the vane natural frequencies are relatively high and the vibrational stress levels low. A detailed finite element analysis is required to further assess this but, based on experience in diffuser mechanical design, it is conceivable that the forward vane portion can be made substantially thinner than current state of the art.

Experimental Assessment

Two different G-series diffusers and the baseline diffuser were assessed experimentally in full-scale compressor tests. The measurements were postprocessed using a proprietary mean-line data reduction scheme to calculate conditions through the compressors. The maximum measurement errors, to within 95% confidence levels, are $\leq \pm 1.0\%$ for flow rate, $\leq \pm 0.2\%$ for total pressure ratio, and $\leq \pm 0.5\%$ for efficiency. The design parameters are summarized in Table 1. While the G designation originated from the

Table 1 Design parameters of experimentally tested diffusers

Design	r_3/r_2	r_4/r_2	AR	r_{LE}/c	r_5/r_2	r_5/r_4
Baseline	1.15	1.40	1.52	N/A	1.63	1.16
G5	1.15	1.44	1.44	0.008	1.63	1.13
G7	1.225	1.50	1.44	0.008	1.63	1.08

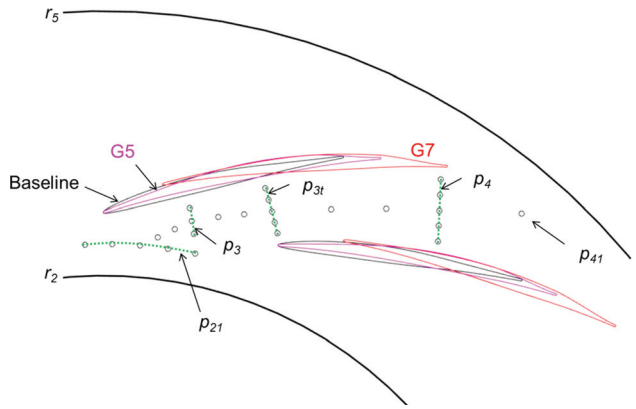

Fig. 18 Illustration of common diffuser measurement plate instrumentation used to assess diffuser subcomponent performance

Gaussian thickness distribution, the number designation is only chronological and has no other significance. The G5 diffuser was designed based on comparable overall design parameters (r_3/r_2, r_4/r_2, and AR) but different leading edge radii. The G7 diffuser was designed to assess the effect of higher inlet radius ratio and shorter downstream vaneless space on diffuser performance. The same volute at $r_5/r_2 = 1.63$ was used for all the diffusers tested.

Figure 18 illustrates the fixed static pressure tap array overlaid with the three different test diffusers. The pressure is pitchwise averaged at diffuser inlet, vane leading edge radius, throat, and vane trailing edge radius (stations 21, 3, 3*t*, and 4, respectively). The midchannel pressure recovery is measured by pressure taps located on the channel centerline from station 21 to 41. The diffuser exit conditions for the G7 diffuser cannot be accurately assessed because the pressure at the diffuser exit radius cannot be pitchwise averaged. Hence, only the midchannel pressure recovery characteristic is shown for G7. The diffuser static pressure recovery along the diffusion path is shown in Fig. 19. The same trend is observed as predicted by the area schedule plots. The flow area reduction in the semivaneless space of the baseline diffuser accelerates the flow. Similarly, the area reduction in the vaneless space of the G7 diffuser generates high profile loss with little diffusion. As more kinetic energy is dissipated in the vaneless space, the diffuser inlet Mach number decreases yielding less pressure recovery. The smooth diffusion path, combined with a higher diffuser inlet Mach number, improves the pressure recovery of the G5 diffuser compared to the baseline diffuser.

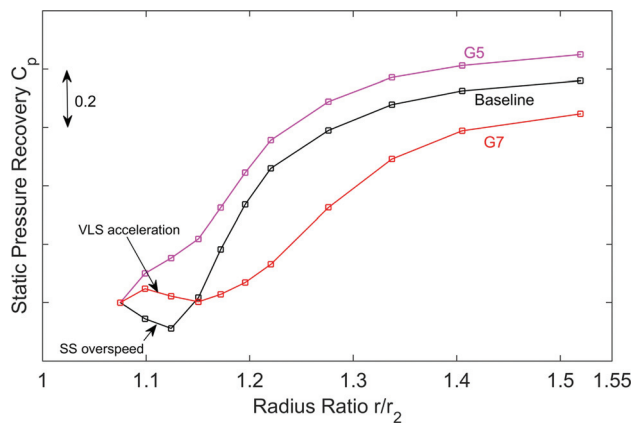

Fig. 19 Measured diffuser channel static pressure rise for baseline, G5, and G7 diffusers. The SVLS of the G5 diffuser provides 12% improvement of overall pressure recovery relative to the baseline diffuser.

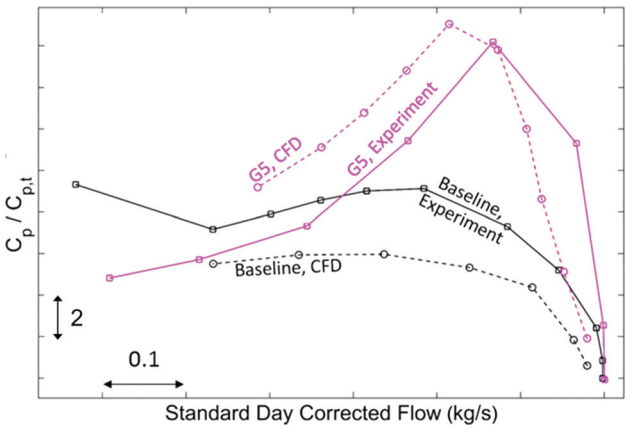

Fig. 20 Comparison of baseline versus G5 diffuser performance parameter $C_p/C_{p,t}$: the baseline RANS calculation overpredicts separation and therefore underpredicts $C_p/C_{p,t}$

Since the baseline and the G-series diffusers have different area ratios, the diffuser performance parameter $C_p/C_{p,t}$ is used to compare diffuser performance. The trends of the mixed-out averaged calculations in Fig. 20 show good agreement with the experimental results, and the G5 diffuser demonstrates a 1.8 fold improvement in $C_p/C_{p,t}$ relative to the baseline case.

The thin leading edge of the G5 diffuser impacts the range of improved diffuser performance. The performance drops back to baseline levels at off-design conditions. This is in agreement with the impeller exit pitchwise unsteady incidence variation observed in Ref. [1]. However, the surge margin is maintained, and a better overall performance is achieved.

In summary, for matched inlet flow angles[7] profile thickness inevitably causes the diffuser area schedule to deviate from ideal. To avoid undesirable flow area reduction, the idea behind the aft-thickened G-series diffuser is to shift the thickness to higher radii such that maximum diffusion can be achieved in the semivaneless space.

Diffusion System Component Interaction

In addition to mechanical challenges, strong pitchwise static pressure variation at impeller exit can lead to decreased impeller performance [9]. The pitchwise static pressure variation due to vane upstream influence can be defined as

$$\frac{\overline{p(\theta)} - \overline{\overline{p_{21}}}}{\overline{\overline{p_{t,21}}} - \overline{\overline{p_{21}}}} \tag{7}$$

where $\overline{\overline{p_{21}}}$ and $\overline{\overline{p_{t,21}}}$ are the time and pitchwise averaged static and total pressures at station 21, and $\overline{p(\theta)}$ is the time-averaged local static pressure.

The vane upstream pressure variations were extracted from the stage RANS calculations and compared with the experimental results. The measurements are assumed periodic and are therefore repeated. The calculations for the baseline diffuser agree well with the experimental results in Fig. 21. For the G5 diffuser in Fig. 22, the peak-to-peak pressure variation is reduced by 42% at best diffuser efficiency. The reduced upstream influence can be attributed to the leading edge shape/thickness, as the thin leading edges in the G5 diffuser cause the detached bow shock in front of the vanes in the baseline diffuser to become attached oblique shocks. The reduced upstream influence mitigates impeller exit pressure nonuniformity and thus improves impeller efficiency.

[7]The diffuser inlet metal angles were matched to the impeller outflow at zero incidence which, as will be shown, occurs at lower corrected flow than peak diffuser performance. This leads to a mismatch between impeller and diffuser and can be corrected in a second design iteration.

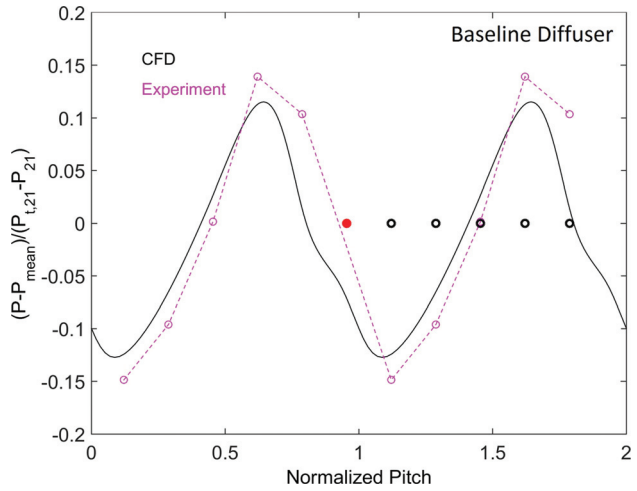

Fig. 21 Pitchwise static pressure variation near baseline diffuser inlet. Pressure tap locations are marked by thick circles. Linear interpolation used for missing pressure tap (marked by solid dot).

Figure 23 compares impeller efficiency between the baseline design and G5 diffuser. The mixed-out averaged calculation agrees in trend with the experimental data. As vane upstream influence attenuates, the impeller efficiency improves by 0.8% points at the design condition relative to the baseline diffuser.

From a stage performance perspective, the G5 diffuser achieves a 0.74% point improvement at design conditions relative to the baseline diffuser in Fig. 24. The measured efficiency improvement is less than that computed, which is suggested to be due to the overpredicted separation in the baseline diffuser calculations. This overprediction is well documented in the literature [8,9]. Figure 25 illustrates the changes in diffusion system isentropic efficiency (including volute) compared to the stage efficiency. In addition to the impeller–diffuser mismatch, the volute contributes significantly to the loss relative to the stage only (dashed lines). The G5 diffuser has a shorter downstream vaneless space which, combined with a higher diffuser exit Mach number, is thought to negatively impact volute performance [8].

To summarize, Fig. 26 illustrates the impact of the volute mismatch on the overall characteristics. The work coefficient is improved due to the reduced vane upstream influence while the overall pressure ratio remains about the same as the G5 diffuser performance benefits are neutralized by the increased volute loss.

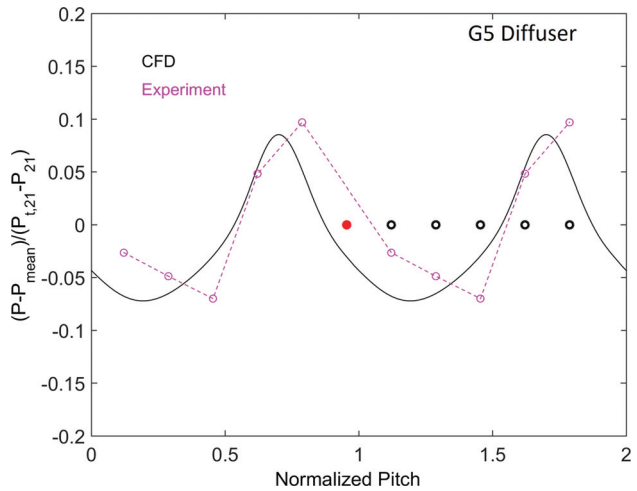

Fig. 22 Pitchwise static pressure variation near G5 diffuser inlet

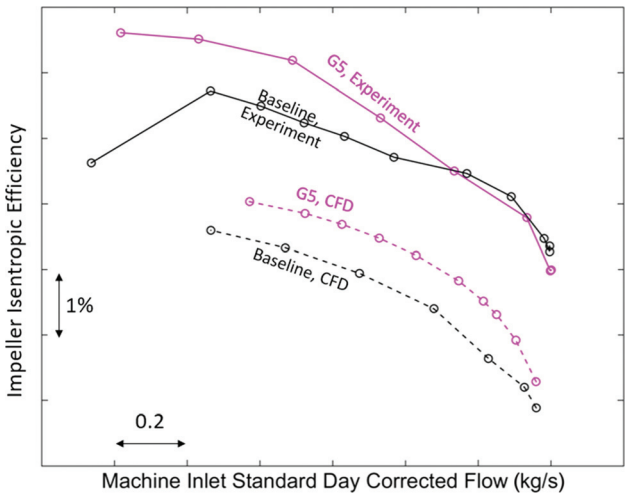

Fig. 23 The G5 diffuser yields a 0.8% point improvement in impeller efficiency relative to the baseline diffuser at design condition

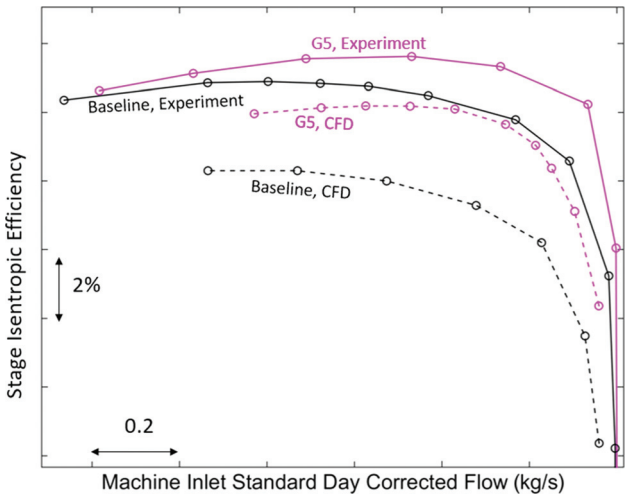

Fig. 24 The G5 diffuser achieves a 0.74% point improvement in stage efficiency relative to the baseline diffuser at design condition

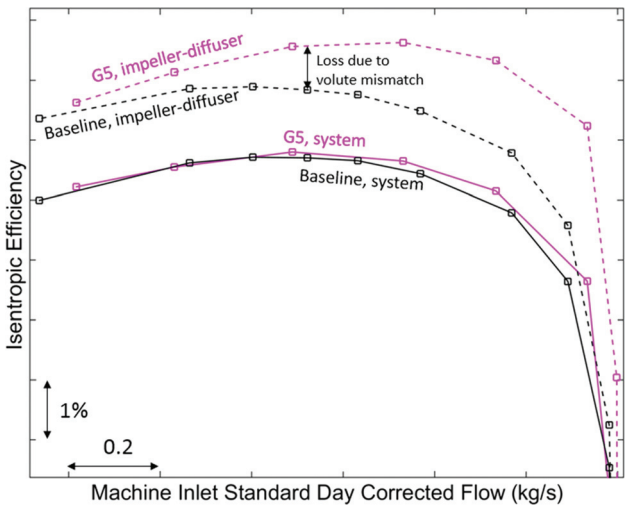

Fig. 25 Stage efficiency compared to diffusion system efficiency (volute included) at design condition: the higher exit Mach number of the G5 diffuser increases volute stagnation pressure loss

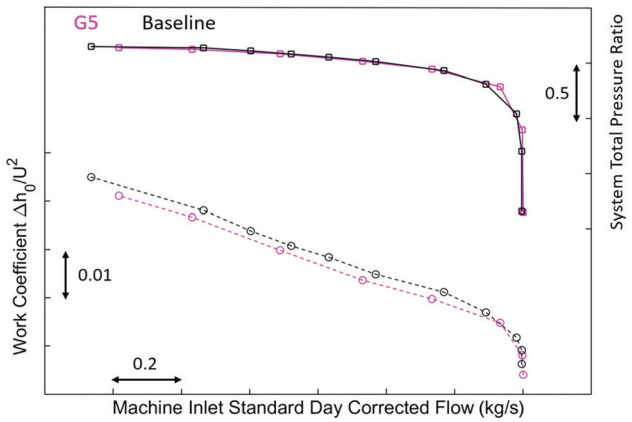

Fig. 26 Work coefficient and system total pressure ratio at design condition

Time and cost did not permit further experiments with a better matched volute. This is left for future work.

Summary and Conclusions

Both computations and experiments demonstrate that a smooth diffusion path, which avoids area reductions and discontinuities, is critical for improved diffuser performance. More specifically, the semivaneless space is the diffuser subcomponent that offers the highest potential for performance improvements by mitigating flow overspeed, reducing profile loss, and increasing effective diffusion length.

Based on the zero-thickness camberline diffuser study, the ideal diffuser performance is set by diffuser area ratio and effective nondimensional diffusion length, governed by the inlet and exit radius ratios and the flow turning angle. A large increase in flow area can lead to flow separation and reduce pressure recovery. Closer-spaced diffuser vanes increase the inlet Mach number and therefore pressure recovery.

Adopting the ideal camberline as the suction side of the profiled diffuser ensures high-pressure recovery at low stagnation pressure loss in the semivaneless space. Thin leading edges enable smooth flow area transition into the diffuser channel and reduce vane upstream influence, yielding higher channel pressure recovery as well as improved impeller efficiency.

The volute performance is hypothesized to be sensitive to both volute inlet swirl parameter and Mach number. A lower volute inlet Mach number is desirable and to achieve performance improvements on the overall diffusion system level, the volute needs to be carefully matched.

The area schedule based G-series diffusers demonstrate improved channel pressure recovery especially in the semivaneless space, where unwanted flow accelerations seen in the baseline diffuser are transformed into continuous diffusion. A 1.8 fold improvement in diffuser performance parameter $C_p/C_{p,t}$ was achieved. In addition, a 0.8% point increase in impeller isentropic efficiency due to reduced vane upstream influence and a 0.74% point increase in stage efficiency were demonstrated.

Acknowledgment

The authors would like to thank Professor Nick Cumpsty for the stimulating discussions and the anonymous reviewers for their useful and constructive comments. Their suggestions have improved the paper greatly. This research was funded by ABB Turbo System, Ltd., which is gratefully acknowledged.

Nomenclature

a = semimajor axis
A = flow area
A_{th} = diffuser total throat area
AR = area ratio
b = semiminor axis
c = vane chord
C_p = pressure recovery coefficient
$C_{p,i}$ = ideal pressure recovery coefficient
$C_{p,t}$ = stagnation pressure loss coefficient
CFD = computational fluid dynamics
HCF = high-cycle fatigue
LE = vane leading edge
m = location of maximum thickness
M = Mach number
p = static pressure
p_t = stagnation pressure
ps = vane pressure side
r = radius
RANS = Reynolds-averaged Navier–Stokes
s = span
ss = vane suction side
SVLS = semivaneless space
T = static temperature
T_t = stagnation temperature
TE = vane trailing edge
V_r = radial velocity
V_θ = tangential velocity
VLS = vaneless space
x = distance along the chord
y^+ = dimensionless wall distance
α = flow angle
ε = eccentricity
ε_D = diffuser effectiveness
η = efficiency
λ = volute inlet swirl parameter
σ = standard deviation

References

[1] Everitt, J., Spakovskzy, Z., Rusch, D., and Schiffmann, J., 2016, "The Role of Impeller Outflow Conditions on the Performance and Stability of Airfoil Vaned Radial Diffusers," ASME Paper No. GT2016-56168.
[2] Reneau, L., Johnston, J., and Kline, S., 1967, "Performance and Design of Straight, Two-Dimensional Diffusers," ASME J. Basic Eng., **89**(1), pp. 141–150.
[3] Japikse, D., and Baines, N., 1998, *Diffuser Design Technology*, Concepts ETI, White River Junction, VT.
[4] Japikse, D., 1996, *Centrifugal Compressor Design and Performance*, Concepts ETI, White River Junction, VT.
[5] Horlock, J. H., 1958, *Axial Flow Compressors, Fluid Mechanics and Thermodynamics*, Butterworths, London.
[6] Faulders, C., 1956, "Aerodynamic Design of Vaned Diffusers for Centrifugal Compressors," ASME Paper No. 56-A-213.
[7] Casey, M., and Rusch, D., 2014, "The Matching of a Vaned Diffuser With a Radial Compressor Impeller and Its Effect on the Stage Performance," ASME J. Turbomach., **136**(12), p. 121004.
[8] Gao, R., 2015, "Area-Schedule Based Design of High Pressure Recovery Radial Diffusion Systems," Master's thesis, Department of Aeronautics and Astronautics, Massachusetts Institute of Technology, Cambridge, MA.
[9] Murray, N., 2003, "Effects of Impeller-Diffuser Interaction on Centrifugal Compressor Performance," Master's thesis, Department of Aeronautics and Astronautics, Massachusetts Institute of Technology, Cambridge, MA.